JOURNAL OF MATERIALS SCIENCE 22 (1987) 4446–4452

Microstructural modifications in a dynamically consolidated microcrystalline nickel–titanium alloy powder

NARESH N. THADHANI
Center for Explosives Technology Research, New Mexico Institute of Mining and Technology, Socorro, New Mexico 87801, USA

THAD VREELAND Jr, THOMAS J. AHRENS
California Institute of Technology, Pasadena, California 91125, USA

Spherically shaped, microcrystalline NiTi alloy powder with both nonhomogeneous particle-size distribution (2 to 60 μm diameter) and chemical composition, was consolidated with a shock input energy of 316 kJ kg^{-1}. Upon shock compaction, the two-phase NiTi powder particles (containing 45 wt% Ti and 65 wt% Ti) were bonded together, generally by interparticle melting and subsequent welding. The melted material at interparticle regions was observed to have rapidly solidified to largely amorphous and/or microcrystalline phases. Particle interiors were also subjected to extensive plastic deformation which resulted in deformation twinning, grain elongation and some recrystallization to defect-free grains. Unique microstructural modifications occurring due to inhomogeneous thermal and mechanical processing during the dynamic consolidation process, are reported here.

1. Introduction

The NiTi alloy is of interest to physicists and metallurgists because of its unusual physical properties and phase changes. It undergoes a martensitic transformation which can give rise to a shape memory effect [1, 2]. At temperatures below the martensite start temperature, the near-stoichiometric NiTi alloy is ductile with a relatively low yield strength. If a wire or sheet of the alloy is deformed in the martensitic state, it will regain the original shape when heated to temperatures above the martensite-to-austenite transition.

A whole range of Ni_xTi_{1-x} phases in the NiTi alloy system also form an amorphous phase by plasma sputtering, chemical vapour deposition and electron beam evaporation from the vapour phase, as well as by rapid solidification from the melt [3, 4]. Certain newer techniques which involve subjecting the crystalline solid Ni_xTi_{1-x} alloy to various types of disordering processes, e.g. irradiating with energetically charged particles have also been adopted for amorphizing Ni_xTi_{1-x} alloys [5, 6].

More recently, elemental polycrystalline nickel and titanium metals have been transformed into amorphous alloy by simple solid state thermal interdiffusion [7]. Based on a similar concept of solid state amorphization, Schwarz *et al.* [8] have produced amorphous Ni_xTi_{1-x} alloys by mechanically alloying elemental mixtures of nickel and titanium metal powders in a high-energy ball mill. An initially homogeneous crystalline NiTi intermetallic alloy has also been transformed to an amorphous state with the same technique. Amorphous alloys have been produced [9, 10] by relatively slow co-deformation of a layered composite of two elemental metals which gives a large cross-sectional reduction ratio.

Most of the techniques described above for producing amorphous materials suffer from the same basic problem of making bulk alloys which are free from size limitations. At least one of the dimensions of the alloy made by this technique has to be less than about 100 μm. Dynamic consolidation of rapidly solidified powders has evolved as a novel process for making bulk amorphous solids without losing or sacrificing the metastable nature of the starting powders [11–15]. In this technique the consolidation of the powder to full solid density occurs by the passage of a single shock wave of sufficient amplitude. Within a short time interval (corresponding to the rise time of the shock wave) [16–18], the energy of the shock is utilized in plastically deforming the powder particles and reducing the void volume to virtually zero. This results in preferential heating which can cause melting of near surface material and interparticle welding.

The heating and melting of particle surfaces occurs in time durations too small for significant atomic diffusion to occur. The melted interparticle material rapidly solidifies (due to heat flow towards relatively cool particle interiors) at rates as high as 10^5 to 10^{10} °C sec^{-1} [13], thereby retaining the metastable microstructures of the parent powders. Vreeland *et al.* [18] have quantitatively shown that during dynamic consolidation of a glass-forming microcrystalline Markomet 1064 ($Ni_{55.8}Mo_{25.7}Cr_{9.7}B_{8.8}$) alloy powder, up to 30% melt is formed at shock input energies of 595 kJ kg^{-1}. Approximately 20% of this melt solidifies

0022–2461/87 $03.00 + .12

sufficiently rapidly to form amorphous material while the rest transforms to a very fine microcrystalline structure. A model of the shock-induced heating, melting, and cooling of powder particles indicated that while the highest shock energy density is input near the particle surfaces, the majority of the energy is expended in plastic deformation of particle interiors.

In the present work, a spherically shaped microcrystalline NiTi alloy powder, having a fairly non-homogeneous particle-size distribution and chemical composition, was dynamically consolidated. The structural features at interparticle regions and within particle interiors in the NiTi compact were investigated using optical and transmission electron microscopy. The unique microstructural modifications developing due to inhomogeneous thermal and mechanical processing and subsequent plastic deformation during the dynamic consolidation process are reported in the following sections.

2. Experimental procedure

Rapidly solidified microcrystalline NiTi alloy powder obtained from Special Metals Inc., New York, was dynamically consolidated by a stainless steel projectile impacting at 950 m sec^{-1}. The spherically shaped NiTi powder particles ranged from 2 to 60 μm in diameter. A scanning electron micrograph of the as-received powder particles is shown in Fig. 1. The NiTi powder particles had two different chemical compositions. Semi-quantitative electron microprobe analysis performed showed that about 60 to 70% of the powder particles had a composition close to Ni–45 wt % Ti and the balance was Ni–65 wt % Ti. Fig. 2 is an optical micrograph of mechanically polished and etched powder particles mounted in lucite, revealing different etching contrast. The Ni–65 wt % Ti particles are finer grained and darker than the coarse-grained and lighter Ni–45 wt % Ti particles.

Shock consolidation was accomplished by impacting a statically pressed powder (distension = 1.8) in a hardened steel container with a propellant-driven

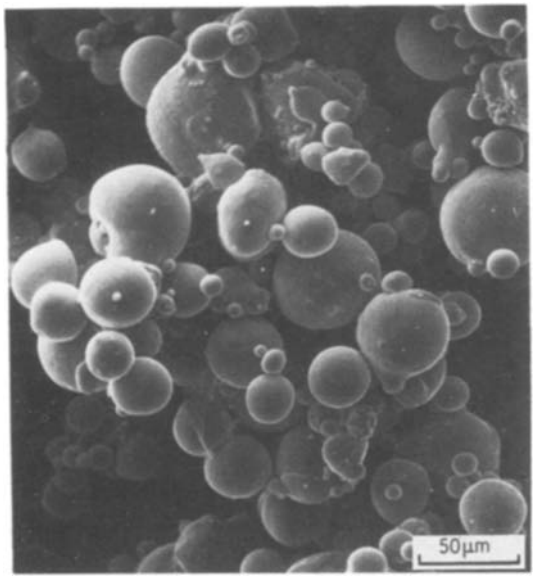

Figure 1 Scanning electron micrograph of the as-received NiTi alloy powder particles.

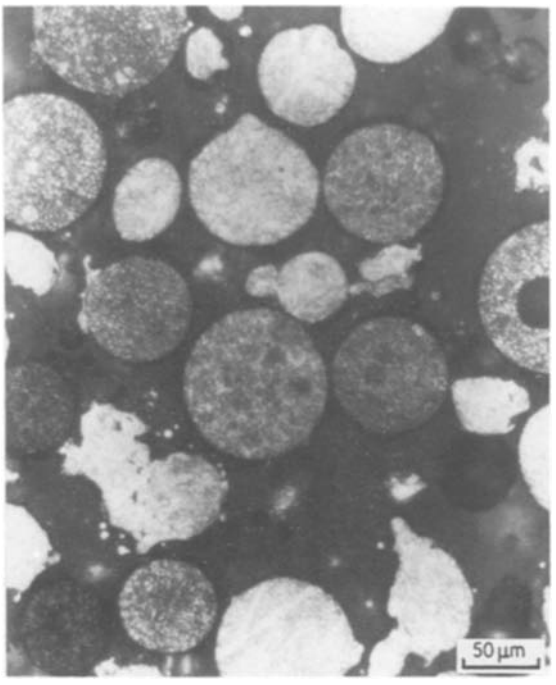

Figure 2 Optical micrograph of mechanically polished and etched NiTi powder particles showing the dark etching and fine-grained Ni–65 wt % Ti particles, and light etching and coarse-grained Ni–45 wt % Ti particles.

AISI 304 SS projectile at a velocity of 950 m sec^{-1}. The 20 mm bore diameter propellant gun at the CalTech Seismological Laboratory was used. The shock pressure using a porous NiTi equation of state (calculated) was ~8.0 GPa. Assuming irreversible compaction, this pressure translates into an internal energy gain (or shock input energy) of 316 kJ kg^{-1}. Details of the experimental set-up are described elsewhere [19,20]. The recovered consolidated NiTi alloy sample (5 mm thick and 20 mm diameter) was sectioned parallel and perpendicular to the direction of shock propagation. Optical and transmission electron microscopy was performed to analyse the structural changes undergone during the compaction process, at interparticle regions and within particle interiors. For optical microscopy and electron-microprobe analysis, the sections were mechanically polished and etched with a solution of 10 ml HF, 20 ml HNO_3 and 150 ml H_2O. Samples for transmission electron microscopy were prepared by cutting 3.0 mm diameter discs from sections mechanically polished to 150 μm thickness. Final thinning was achieved by twin-jet electro-polishing with 70% methanol and 30% nitric acid at −55° C and 20 V. A Philips EM 420 TEM/STEM was used for electron imaging and diffraction analysis.

3. Results and discussion

The spherically shaped NiTi alloy powder was consolidated to full solid density by a planar shock front with energy of 316 kJ kg^{-1}. The microcrystalline powder particles were generally bonded together by the interparticle melt which solidified to either an amorphous or microcrystalline phase, or a mixture of both. Fig. 3 shows optical micrographs of well-bonded powder compacts taken in the plane of shock (Fig. 3a) and on a perpendicular section (Fig. 3b). The dark etching

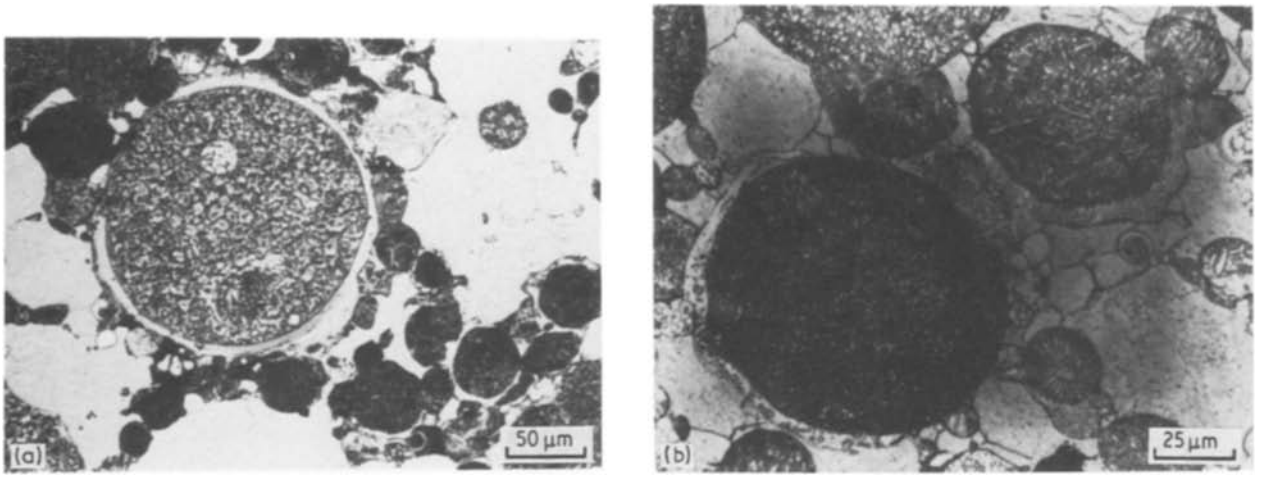

Figure 3 Optical micrographs of shock-consolidated NiTi powder compacts (a) in the plane of shock, and (b) along the perpendicular section.

contrast of the fine-grained Ni–65 wt % Ti and light etching contrast of the Ni–45 wt % Ti particles is evident in the optical micrographs. Also seen in the two micrographs is an almost uniform layer of light contrast material surrounding the bigger Ni–65 wt % Ti particles. An approximate microprobe analysis of the material in the light-contrast layer showed that it contained up to 53 to 60 wt % Ti and balance nickel. A light contrast layer was not observed in the as-received powder particles, hence it is believed to have formed during the consolidation process.

In general, good interparticle bonding was observed in the NiTi powder compact. The strength of the bond is evident by some isolated intraparticle cracking observed in an optical micrograph taken along a cross-sectional plane shown in Fig. 4. The cracking is attributed to the interaction of waves reflecting from lateral surfaces of the steel container.

3.1. Characteristic features at interparticle regions

During the process of dynamic consolidation, the energy of the shock is deposited very inhomogeneously at particle surfaces and within particle interiors. Various models on preferential energy deposition at particle surfaces have been formulated [11, 13, 18, 21], based on heat-flow concepts in very simplified spherical geometries. In a system having a wide distribution of particle sizes and chemical composition, the actual energy deposition in a region of the compact depends upon the size, composition, and distribution of particles in the region. This makes it difficult to predict the amount of melting which will occur during consolidation. However, based on the simplified model by Vreeland *et al.* [18] about 10% melting was estimated in the NiTi alloy consolidated at 316 kJ kg^{-1}. No attempt was made to measure the amount of melt in the consolidated NiTi alloy, but the micrographs suggest that approximately 10% of the structure had melted.

The melted regions were generally non-uniform and appeared to be scattered inhomogeneously between particles, depending on the size and type of particles in contact with one another. Different characteristic features were observed at interparticle regions, using transmission electron microscopy ranging from no evidence of melting to localized melting and rapid solidification to amorphous and/or microcrystalline structure. The characteristic features will be described next.

Some particles with dissimilar phases which were in contact with one another showed an absence of significant interparticle melting (less than a few atomic layers). Fig. 5 is a bright-field TEM image

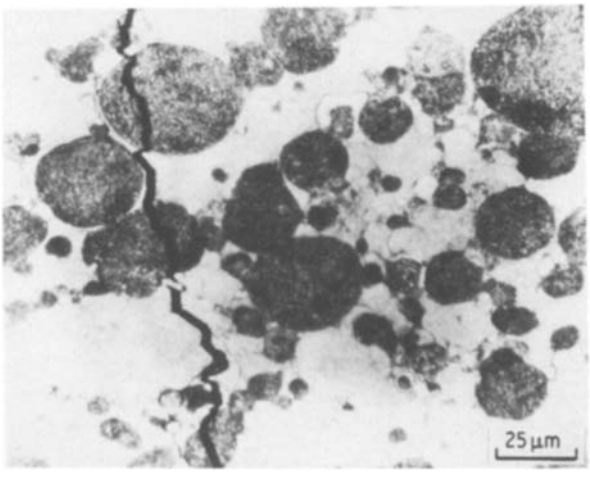

Figure 4 Optical micrograph of consolidated NiTi powder in perpendicular section revealing intraparticle cracking.

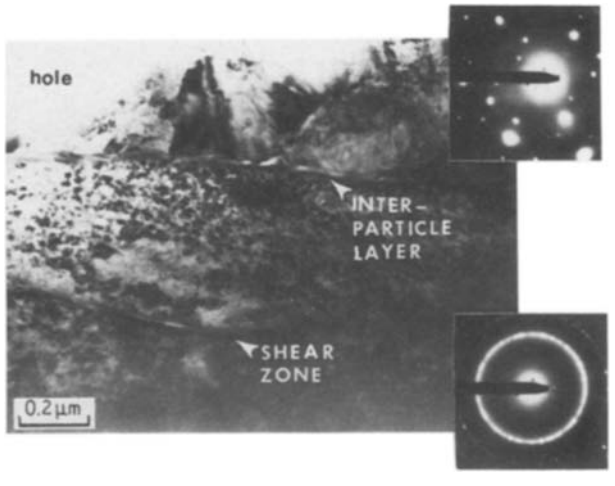

Figure 5 Bright-field transmission electron micrograph showing Ni–65 wt % Ti and Ni–45 wt % Ti particles separated by a 10 nm thick interparticle layer.

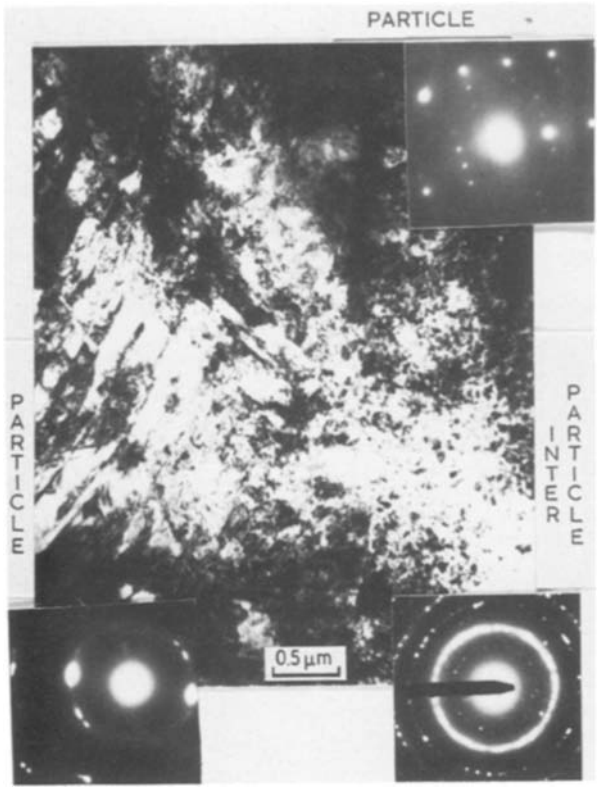

Figure 6 Transmission electron micrograph showing fine microcrystalline grains at the interparticle region.

showing Ni–65 wt % Ti (fcc, $a = 1.1345$ nm) and Ni–45 wt % Ti (bcc, $a = 0.2980$ nm) particles and a 10 nm thick interparticle layer. The respective diffraction patterns confirm that the particles are not of the same phase. The narrow white contrast band in the fine-grained Ni–65 wt % Ti particle is interpreted as a region of intense shear localization.

An example of an interparticle region consisting of very fine microcrystalline grains (0.04 μm grain diameter), is shown in the bright-field TEM image in Fig. 6 (running diagonally in the image plane from top left-hand side to bottom right-hand side). The diffraction pattern of the interparticle material confirms the very fine grain size which presumably formed by a rapid quench of melted material. The particle to the left of the interparticle region shows elongated grains resulting from extensive plastic deformation. Elongated grains are generally observed close to the interparticle regions.

Clear evidence of interparticle melting is shown in the bright-field electron micrograph in Fig. 7. The light and clear contrast region at the centre of the micrograph is the interparticle material that melted and subsequently resolidified to an amorphous structure (confirmed by the diffuse SAD ring pattern, (A)). This interparticle material is believed to have the same chemical composition as the bright contrast material

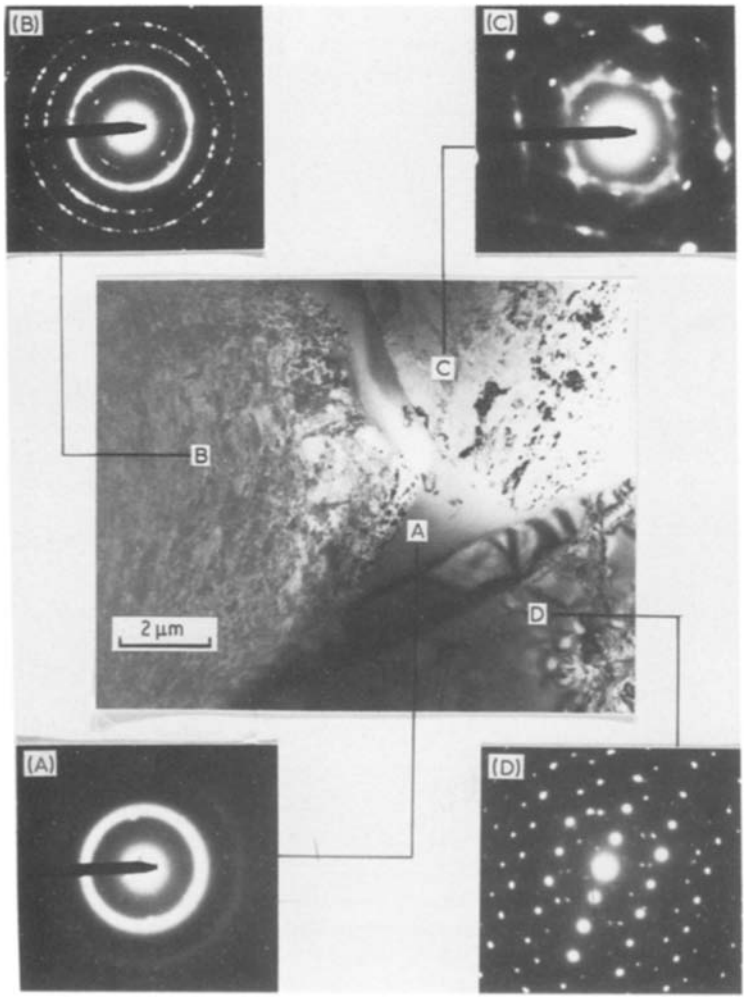

Figure 7 Transmission electron micrograph of interparticle region containing amorphous material formed upon rapid solidification of the melt, surrounded by dissimilar phase particles.

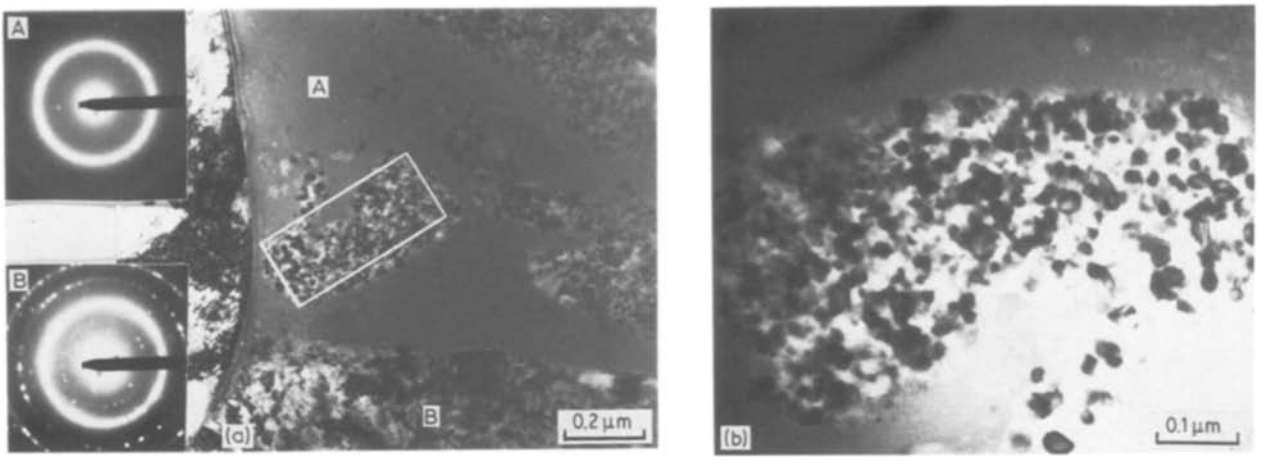

Figure 8 (a) Transmission electron micrograph showing the presence of both amorphous and microcrystalline material formed from the melt at interparticle regions, and (b) higher magnification view of the insert in (a).

(53 to 60 wt % Ti, balance nickel) in the layer surrounding the Ni–65 wt % Ti particles in Fig. 3. However, no conclusive test with energy dispersive X-ray microanalysis was performed to confirm the composition. It is well known that the $NiTi_2$ phase is an easy glass former compared to the NiTi phase [22]. The present investigation also suggests that most of the melted and resolidified material that transforms to metallic glass has a composition close to $NiTi_2$ and not the NiTi phase.

The regions marked B and C in the micrograph in Fig. 7 correspond to the Ni–65 wt % Ti (fcc, a = 1.1345 nm) and Ni–45 wt % Ti (bcc, a = 0.2980 nm) particles respectively, as confirmed by the SAD patterns (B) and (C). The region marked D is part of the Ni–65 wt % Ti particle that was subjected to considerable plastic deformation during the consolidation process, but did not melt; instead the extensive deformation and heating resulted in recrystallization of the Ni–65 wt % Ti fcc grains. The lattice parameter of the recrystallized fcc grains was determined to be 1.1310 nm. More examples of such deformation-induced recrystallization will be discussed later.

In certain interparticle regions, the melt pools formed were quite large. The material in the middle of these larger melt pools did not solidify at a fast enough rate to form metallic glass, but instead nucleated and grew fine microcrystalline grains. Fig. 8a is a bright-field TEM image showing fine microcrystalline grains surrounded by amorphous material at an interparticle region. The respective diffraction patterns confirm the amorphous and microcrystalline structures. The microcrystalline grains (0.02 to 0.04 μm diameter) do not show evidence of plastic deformation, but exhibit crystallization twinning (as seen in Fig. 8b (which is a higher magnification view of the insert in 8a)), which

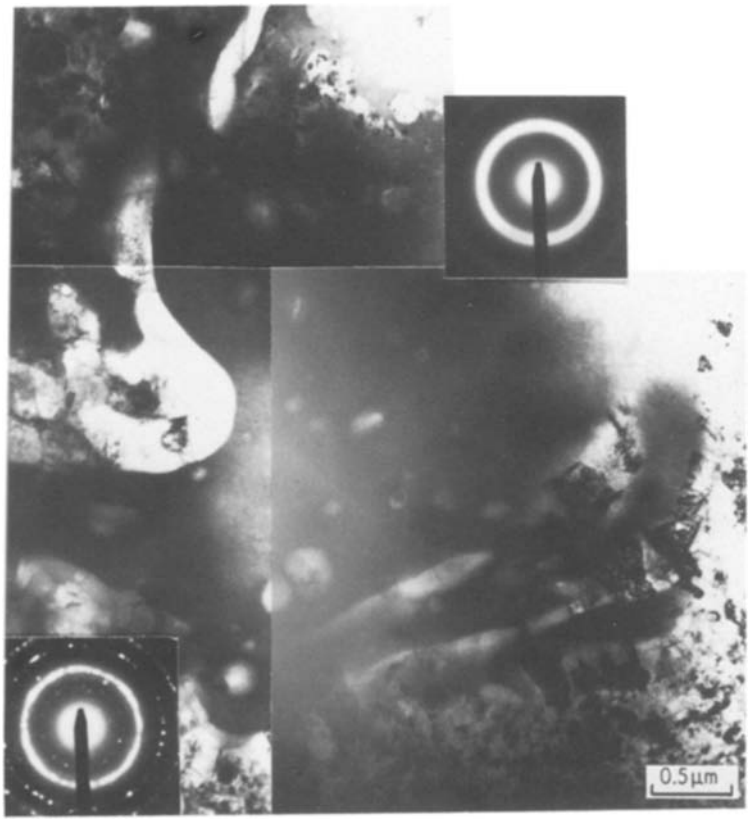

Figure 9 Transmission electron micrograph showing amorphous material at interparticle regions and containing a dispersion of unmelted oxide contaminations.

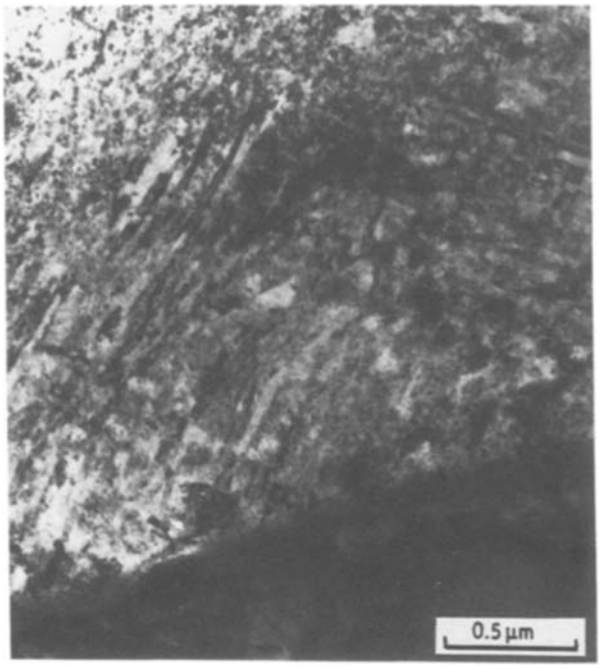

Figure 10 Bright field transmission electron micrographs showing evidence of deformation twinning resulting from plastic deformation of particle interiors.

indicates that the grains were formed upon solidification of the melt during compaction. Similar formation of microcrystalline and amorphous material upon solidification from the melt has also been observed in the investigations of Vreeland *et al.* [18, 19].

In cases where the NiTi particle surfaces were contaminated with oxides, the melted material at interparticle regions consisted of a dispersion of unmelted oxides. Fig. 9 shows amorphous material formed at interparticle regions and containing possibly unmelted oxides. Although care was taken in minimizing the oxygen contamination of the NiTi powder during loading of the target and the compaction experiment, it is believed that the as-received powder had some contamination.

3.2. Deformation features within particle interiors

A considerable amount of energy is deposited near particle surfaces resulting in melting of near surface material. But, it has also been shown [18] that a non-negligible amount of shock energy is utilized in plastic deformation of particle interiors. The deformation is generally manifested in the form of slip or twinning, although other examples of non-homogeneous plastic deformation due to shear localization have also been reported [23].

In the present case for the NiTi alloy, deformation twinning and elongated grains were observed. In some particles, plastic deformation also resulted in recrystallization of the grains as is seen in Fig. 7. Examples of grain elongation and deformation twinning are shown in Figs 6 and 10, respectively. If the deformation is localized within particle interiors, the extensive heat generated due to plastic deformation can result in recrystallization of some of the grains within the particles. Recrystallization is most likely to occur in heavily deformed particles located in regions of the compact where the initial distension was high. Characteristic microstructures revealing fully annealed substructure of such recrystallized grains are shown in Figs 11a and b. The micrograph in Fig. 11b shows a region of deformation twins which did not recrystallize and thus retained segments of the original twins (indicated by arrows).

These unique structural modifications reveal the extremely inhomogeneous thermal and mechanical processing experienced by the powder particles within particle interiors and at interparticle regions, during the shock consolidation process.

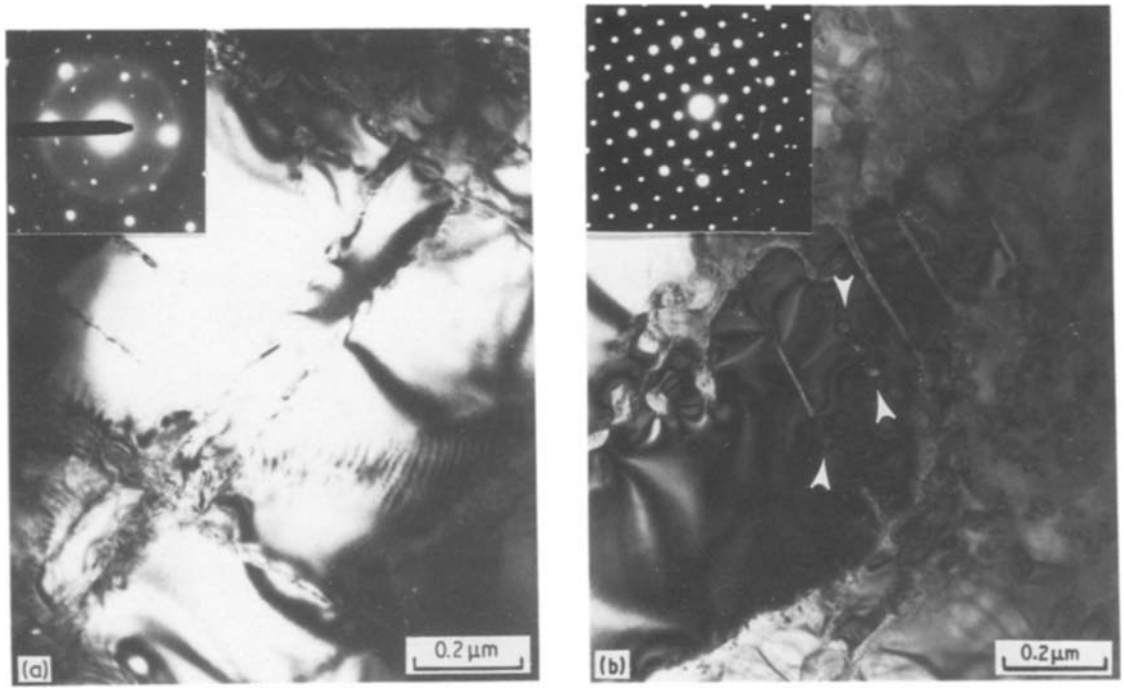

Figure 11 (a, b) Transmission electron micrographs showing recrystallized grains due to extensive plastic deformation and heating of particle interiors.

4. Conclusions

1. Two-phase NiTi alloy powder particles (containing 45 wt % Ti and 65 wt % Ti) having a size range of 2 to 60 μm diameter were shock consolidated at an impact velocity of 950 m sec^{-1}.

2. Upon consolidation the powder particles were well-bonded, generally by interparticle melting. The amount of melt formed at 316 kJ kg^{-1} shock energy was approximately 10%.

3. Evidence of bonding between particles of dissimilar compositions with little or no interparticle melting was also observed.

4. The melted material at interparticle regions rapidly solidified to an amorphous phase or to a very fine microcrystalline phase.

5. The bulk composition of the material in the interparticle region was estimated to contain up to 60 wt % Ti with the balance being nickel.

6. The oxide contaminants on particle surfaces remained unmelted and were observed as dispersoids in regions which solidified to an amorphous structure.

7. Particle interiors were also subjected to extensive plastic deformation which resulted in the formation of deformation twins, elongated grains and some recrystallization to relatively defect-free grains.

Acknowledgements

This work was supported in part by the National Science Foundation under grant no. DMR-8315214 and the CalTech Program in Advanced Technologies sponsored by Aerojet General, General Motors, GTE, and TRW. The NiTi alloy powder was obtained from Special Metals Corporation, New Hartford, New York. We thank Michael A. Long for help with the compaction experiments and Randy Heuser for performing the EMPA work. CalTech Division of Geological and Planetary Sciences Contribution no. 4434.

References

1. J. PERKINS (ed.), "Shape Memory Effects in Alloys" (Plenum, New York, 1975).
2. C. M. JACKSON, R. J. WAGNER and R. J. WASILEWSKI, "NiTi Shape Memory Alloys", NASA Report No. NASA-SR-5110, (1972).
3. N. J. GRANT and B. C. GIESSEN (eds), Proceedings of Second International Conference on Rapidly Quenched Metals, Sections I and II (M.I.T., Cambridge, Mass., 1976).
4. J. J. GILMAN and H. J. LeEAMY (Eds), "Metallic Glasses", ASM Materials Science Seminar Series (ASM, Metals Park, Cleveland, Ohio, 1977).
5. K. C. RUSSELL, *Prog. Mater. Sci.* **28** (1985) 229.
6. H. MORI, H. FUJITA and M. FUJITA, *Jpn J. Appl. Phys.* **22** (1983) 194.
7. W. L. JOHNSON, B. DOLGIN and M. VAN ROSSUM, in "Glass-Current Issues", edited by A. F. Wright and J. Dupay (Nata ASI Series, E-92, Martinus Nijhoff, Boston, 1985) p. 172.
8. R. B. SCHWARZ, R. R. PETRICH and C. K. SAW, *J. Non-Cryst. Solids* **76** (1985) 281.
9. M. ATZMON, J. R. VEERHOVEN, E. R. GIBSON and W. L. JOHNSON, *Appl. Phys. Lett.* **45** (1984) 1052.
10. L. SCHULTZ, Proceedings Fifth International Conference on Rapidly Quenched Metals, edited by S. Steeb and H. Warlimont (North Holland, Amsterdam, 1985) p. 1585.
11. W. G. GOURDIN, *Prog. Mater. Sci.* **30** (1986) 39.
12. V. F. NESTERENKO, *Frizka Goreniya i vzryva* (1983) 145.
13. D. G. MORRIS, *Metal Sci.* **16** (1982) 457.
14. D. RAYBOULD, *J. Mater. Sci.* **16** (1981) 16.
15. P. KASIRAJ, D. KOSTKA, T. VREELAND Jr and T. J. AHRENS, *J. Non-Cryst. Solids* **61/62** (1984) 967.
16. R. B. SCHWARZ, P. KASIRAJ, T. VREELAND Jr and T. J. AHRENS, *Acta Metall.* **32** (1984) 1243.
17. R. B. SCHWARZ, P. KASIRAJ and T. VREELAND Jr, in Proceedings of International Conference on Metallurgical Applications of Shock Wave and High-Strain-Rate Phenomena, edited by L. E. Murr, K. P. Staudhammer and M. A. Meyers (Marcell Dekker, New York, 1986) p. 313.
18. T. VREELAND Jr, P. KASIRAJ, A. H. MUTZ and N. N. THADHANI, in [17] p. 231.
19. N. N. THADHANI, A. H. MUTZ, P. KASIRAJ and T. VREELAND Jr, in [17] p. 237.
20. T. J. AHRENS, N. N. THADHANI, A. H. MUTZ, T. VREELAND Jr, R. B. SCHWARZ, J. A. TYBURCZY, S. L. M. SHASTRI and T. C. PENG, in [17] p. 83.
21. K. KONDO, S. SOGA, A. SAWAOKA and M. ARAKI, *J. Mater. Sci.* **20** (1985) 1033.
22. R. W. CAHN, *Contemp. Phys.* **50** (1980) 6348.
23. N. N. THADHANI and T. VREELAND Jr, *Acta Metall.* **34** (1986) 2323.

Received 20 February
and accepted 29 Arpil 1987